Article

Surface Smoothing by Gas Cluster Ion Beam Using Decreasing Three-Step Energy Treatment

Vasiliy Pelenovich [1,2], Xiaomei Zeng [2,*], Xiangyu Zhang [2], Dejun Fu [3], Yan Lei [2,*], Bing Yang [2,4] and Alexander Tolstoguzov [3,5,6,*]

[1] Institute of Technological Sciences, Wuhan University, Wuhan 430072, China; v.pelenovich@whu.edu.cn
[2] School of Power & Mechanical Engineering, Wuhan University, Wuhan 430072, China; johnny_zxy@whu.edu.cn (X.Z.); toyangbing@whu.edu.cn (B.Y.)
[3] Wuhan University Shenzhen Research Institute, Nanshan Hitech Zone, Shenzhen 518057, China; djfu@whu.edu.cn
[4] International Joint Research Center for Surface and Interface Materials Science and Engineering, Wuhan University, Wuhan 430072, China
[5] Utkin Ryazan State Radio Engineering University, Ryazan 390005, Russia
[6] Centre for Physics and Technological Research (CeFITec), Universidade Nova de Lisboa, 2829-516 Caparica, Portugal
[*] Correspondence: zxmwuhan@whu.edu.cn (X.Z.); leiyan.material@whu.edu.cn (Y.L.); a.tolstoguzov@fct.unl.pt (A.T.)

Abstract: A three-step treatment of Si wafers by gas cluster ion beam with decreasing energy was used to improve the performance of surface smoothing. First, a high energy treatment at 15 keV and an ion fluence of 2×10^{16} cm^{-2} was used to remove initial surface features (scratches). Next, treatments at 8 and 5 keV with the same fluences reduced the roughness that arose due to the formation of morphological features induced by the surface sputtering at the first high energy step. The surface morphology was characterized by the atomic force microscopy. The root mean square roughness R_q and 2D isotropic power spectral density functions were analyzed. For comparison, the smoothing performances of single-step treatments at 15, 8, and 5 keV were also studied. The lowest roughness values achieved for the single and three-step treatments were 1.06 and 0.65 nm, respectively.

1. Introduction

Gas cluster ion beam (GCIB) technology and its application have made great progress in the past decades [1–3], including micromachining ion beam etching [4], the doping of semiconductor materials [5], ion beam assisted deposition [6], material surface smoothing and planarization [7–10], and self-assembled surface features (nanoripples) formation at off-normal irradiation [11].

The gas cluster is a nanoscale particle that is composed of a few units up to many thousands of atoms or molecules. The gas cluster can be ionized, for example, by means of electron ionization. Due to Coulomb forces that appear in the ionized cluster, which tend to destroy it [12], and weak Van der Waals bonding between cluster atoms, the cluster positive charge cannot exceed seven [13]. It results in a high mass-to-charge ratio in the cluster ion. Since they are accelerated, such cluster ions demonstrate strictly different properties when they interact with solid surfaces compared to monoatomic ion beams [14]; features include high energy density and temperature in the impact region [15], lateral sputtering [16], high sputtering efficiency [17], and surface nanostructuring [18]. Due to the low value of the energy per atom, all cluster surface effects occur in a very shallow surface layer of about ten nm, which means that the cluster treatment is a very mild process that minimizes defect

formation in the target material [19,20]. A high sputtering rate, smoothing effect, and low defect formation make GCIB a very suitable tool for surface modification.

The most developed applications of GCIB are smoothing and planarization of the surface. The root mean square (RMS) roughness R_q of the surface in that case can be reduced to the order of one Å [21]. The mechanism of smoothing was revealed by molecular dynamics (MD) and Monte Carlo simulations [14,22]. It was shown that when keV energy cluster ions bombard the target surface, the sputtering rate of a protuberance area was much higher than that of a concave area. Such quick erosion of the protrusions results in the observed smoothing of the surface. A detailed process of a cluster ion collision with a flat surface was also simulated by MD [23].

A large number of atoms in the cluster ion results in astonishing differences in cluster ion and monoatomic ion interactions with a solid, which means that physically, the interaction between the cluster and target atoms becomes highly non-linear in comparison to the "linear" processes described by Sigmund's collision theory [24]. This theory states that the interaction between a given cluster atom and a target atom depends on the presence of other cluster atoms nearby. During multiple collisions between cluster atoms and target atoms, the nuclear stops in a confined volume, which is comparable with the cluster volume and results in a quick rise in the pressure and temperature in the impact zone, the development of a thermal spike [25], and then the ejection of vaporized and liquid target material from the surface. At a certain energy and cluster size, such a collision is accompanied by a crater formation [2]. This is a specific and inevitable defect of the cluster–surface interaction, which contributes to the minimal roughness of the treated surface. The crater consists of the central pit, the bottom of which is lower than the average surface level, and the crater rim, which is higher than the average surface level [26]. Gspann [27] has shown that the size (including the radius or depth) of a crater formed by a cluster impact can be estimated by an empirical formula which describes the formation of a crater at the hyper-velocity impact of a macroscopic projectile:

$$r = 1.45\sqrt[3]{\frac{E}{B}}, \tag{1}$$

where E is the cluster energy in eV and B is the Brinell hardness of the target [27]. The applicability of Equation (1) at the nanoscale was also demonstrated by the MD simulation of a cluster–surface collision [28].

Hence, one can conclude that in order to decrease the sizes of the craters and therefore improve the final roughness, it is necessary to decrease the energy of the clusters. However, MD simulation performed for Ar_{2000} clusters with different energy has shown that at a low energy limit, Equation (1) is inapplicable; for example, at the energy of 4 keV, the cluster impact does not cause any damage to the Si surface [23], which also means that such low energy clusters are useless for the sputtering of protrusions since their sputtering rate is very small. The sputtering rate Y at a lower energy (<20 keV) can be described by a power function [29]:

$$Y = N[E/(AN)]^q, \tag{2}$$

where N is the number of atoms in the cluster and $A = 57$ eV and $q = 2.25$ are the fitting parameters. The trade-off between the sputtering rate (or time) and the final roughness was observed experimentally for smoothing of the Ta surface [30]. The results show that the surface roughness is reduced most effectively by 28 keV cluster bombardment, while the final average roughness $R_a = 1.6$ Å becomes the lowest after 14 keV treatment.

In addition to the low sputtering rate with low cluster energy, there is the problem of reducing the cluster current at a low accelerating voltage [31] due to the Coulomb repulsion between cluster ions within the beam. Both factors make the smoothing process at low energy time-consuming.

In above-mentioned MD simulations and experimental research, a single energy treatment mode was applied. In this study, to further improve the performance of smoothing

by GCIB, we used a multi-step decreasing energy treatment. In such a smoothing process, a higher energy treatment is necessary to quickly remove the initial rough morphology, whereas subsequent lower energy steps are required to diminish the morphology formed by the cluster impacts of the previous steps. The obtained results are of significance to increase the efficiency of the GCIB treatment of solid-state surfaces.

2. Materials and Methods

For sample preparation, n-Si (100) wafers (KMT Corp., Hefei, China) were used. The roughness of the Si wafer surface was 0.15 nm which was too low for the aim of this study. Therefore, to model a suitable rough surface, we performed a mechanical treatment using a diamond paste with a particle size of 1 μm. After the treatment, the samples were immersed in 10% HF solution to remove the native oxide layer; subsequently, they were ultrasonically cleaned in acetone and deionized water for 5 min.

The working principle and design of the GCIB source used in this study was described elsewhere [32]. A gas source of argon (99.999%) at a pressure of 10 bar supplied a metal supersonic conical nozzle with a throat diameter of 65 μm and an opening angle 2α of 6 deg. The gas pressure in the nozzle chamber was 1 Pa. The ionizing electron energy and emission current were set at 175 eV and 5 mA, respectively. The gas pressure in the sample chamber was 4×10^{-3} Pa (with a full gas supply). The mean cluster specific size was 1000 atoms, and the cluster current at an accelerating voltage of 8 kV was 2 μA.

The Si samples were cut into $4 \times 4 \times 0.5$ mm^3 plates, placed on a sample holder, and irradiated by the cluster beam at a normal incidence. Single-step and three-step energy gas cluster treatments were used. At the single-step mode, the samples were irradiated by 5, 8, or 15 keV cluster ions at fluences of 6×10^{16} cm^{-2}. At the three-step mode, three consecutive treatments at decreasing energies of 15, 8, and 5 keV and equal fluences of 2×10^{16} cm^{-2} (total fluence of 6×10^{16} cm^{-2}) were carried out (Table 1).

Table 1. Energy, ion fluence, and treatment time by the GCIBs, and the roughness of the treated Si surfaces.

Cluster Energy E, keV	Ion Fluence D, $\times 10^{16}$ cm^{-2}	Treatment Time, min	Roughness R_q (10×10 μm^2), nm	Roughness R_q (0.3×0.3 μm^2), nm
Initial surface	-	-	1.69	0.51
15	6	15	1.64	2.39
8	6	12	1.06	1.55
5	6	20	1.15	1.19
15-8-5	2-2-2	5-4-7	0.65	0.87

To study the smoothing of the surface morphology after the gas cluster treatment, an atomic force microscope (AFM) Shimadzu SPM-9500J3 was used. The AFM was operated in the tapping mode with measuring areas of 10×10 μm^2 and 0.3×0.3 μm^2. The RMS roughness R_q and 2D isotropic power spectral density (PSD) function were averaged over 2–3 samples and calculated using NanoScope Analysis code. The measurement roughness inaccuracy did not exceed ± 0.05 nm.

3. Results and Discussion

A representative AFM image of the initial mechanically treated Si surface is shown in Figure 1a. Characteristic scratches with a depth of 3–10 nm and a width of 50–300 nm are observed. The RMS roughness R_q of the mechanically treated surface is 1.69 nm (Table 1).
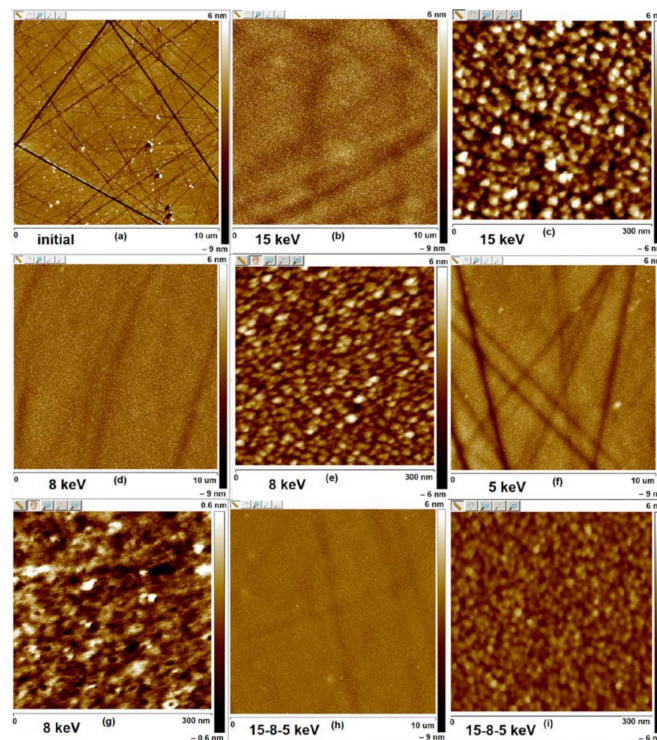
Figure 1. AFM images of: (**a**) the initial mechanically treated Si surface; (**b**,**c**) after Ar cluster treatment at 15 keV, (**d**,**e**) 8 keV, (**f**) 5 keV, and (**g**) 8 keV at an early stage of treatment with a dose of $2.35 \cdot 10^{13}$ cm^{-2}; and (**h**,**i**) after three-step Ar cluster treatment at 15, 8, and 5 keV.

Figure 1b,d,f show the surface morphology of the samples after a single-step treatment with cluster energies of 15, 8, and 5 keV, respectively. Only traces of the deepest scratches are visible after bombardment with 15 keV cluster ions (Figure 1b). Although the smoothing effect is very significant, no reduction in roughness, $R_q = 1.64$ nm, is observed within the experimental uncertainty range (Table 1). The unchanged roughness can be explained by the competition between the smoothing effect and the roughening effect at a nanometer scale. This roughening effect should be connected with the cluster induced surface sputtering, which results in the formation of the surface morphology shown in the AFM image at a higher magnification (Figure 1c).

Figure 1g demonstrates a surface at an early stage of the bombardment with 8 keV cluster ions at a dose of $2.35 \cdot 10^{13}$ cm^{-2}. On the surface, 20 nm craters can be observed. The dose of $2.35 \cdot 10^{13}$ cm^{-2} corresponds to about 100 impacts per crater area; therefore, the craters should be heavily overlapped. However, the "fresh" individual craters are still visible. At a higher dose of $6 \cdot 10^{16}$ cm^{-2} with the surface treated at 15 keV, similar craters are not observed (Figure 1c). It can be due to the well-developed surface morphology induced by the sputtering, which complicates the formation and observation of craters. After the 8 keV treatment (Figure 1d,e), due to the less developed surface morphology, the R_q reduces down to 1.06 nm. A further reduction in the cluster energy to 5 keV at the selected fluence (Figure 1f) shows that such treatment cannot remove the deep scratches and the R_q slightly increases to 1.15 nm.

In order to estimate the effect of the cluster energy on the morphology induced by the sputtering, we calculated the roughness within a measuring area of 0.3×0.3 μm^2, far from the deepest scratches (Table 1). The R_q decreases along with a decrease in the cluster energy. Therefore, we can conclude that the final roughness of the surface is defined by two competing processes. The first one is the smoothing effect, which is more effective at a higher energy and is responsible for the surface planarization. The second process is the surface roughening at the nanoscale, which is induced by the surface sputtering and becomes more evident at a higher energy.

It should be noted that at a high enough fluence, the final roughness tends to be a roughness of the morphology induced by the surface sputtering [30]. However, for low energy GCIB, which can realize negligible induced morphology, the required fluence is very high due to the low sputtering rate. Besides, the cluster beam current at such energies becomes small. Both factors make smoothing at a low energy very time-consuming. To overcome these shortcomings, we have proposed a three-step energy treatment. The first high energy step is necessary to quickly smooth the initial rough surface, and the subsequent lower energy steps reduce the roughness of the surface morphology induced by the previous steps. Figure 1h,i show the Si surface treated subsequently by 15, 8, and 5 keV cluster ion beams at equal fluences of 2×10^{16} cm^{-2} (Table 1). The surface morphology demonstrates weak traces of the scratches (Figure 1h) and the lowest roughness R_q of 0.65 nm (Table 1). These results prove the applicability of the subsequent surface treatment by the cluster beam with decreasing energy.

The results obtained from the triple treatment are comparable with a double Ar/O$_2$ GCIB treatment of poly-SiC wafers [33]. It is shown that 20 keV Ar GCIB can effectively remove surface scratches; however, the RMS roughness increases from an initial 0.3 to 0.7 nm due to asperities formation. A treatment of 10 keV O$_2$ reduces the number of asperities and roughness to 0.3 nm. Lower energy in the O$_2$ treatment does indeed indicate an improvement in the smoothing; however, the reactive nature of the second treatment complicates the process and results in the formation of a ~10 nm oxide layer. Moreover, the relationship between the contributions of the surface sputtering and growth of the oxide layer in the final roughness is not clear.

The RMS roughness cannot provide comprehensive information about the surface morphology. The power spectral density (PSD) function provides more information. The PSD function reveals the distribution of periodic or random morphological characteristics as a function of frequency or wavelength. In Figure 2, the 2D isotropic PSD functions corresponding to the AFM images in Figure 1b,d,f,h are shown. After 15 keV GCIB treatment, the PSD curve decreases to a range of 0.1–1 μm compared with the initial surface, which demonstrates effective smoothing of the scratches. However, at wavelengths less than 0.1 μm, the roughening effect takes place due to the formation of induced morphology. The 8 keV treatment demonstrates better smoothing at wavelengths lower than 0.1 μm, which should be interpreted as the formation of less developed induced morphology, whereas the effectiveness of the scratch removal is similar to that one of the 15 keV treatment. The 5 keV treatment, compared to 15 keV, exhibits less effective smoothing at wavelengths higher than 0.4 μm due to a lower sputtering rate, which correlates with the observation of the residual scratches in Figure 1f. In contrast, the 5 keV treatment shows a substantial improvement in the smoothing in the lower wavelength region. Finally, the PSD function of the three-step energy treatment combines the advantages of a high energy treatment, which effectively removes scratches, and a low energy treatment, which forms less developed induced surface morphology.

In this study, for the three-step energy surface treatment, we used equal fluences. However, it should be noted that the material layer that needs to be sputtered to achieve a smoothing effect is usually about 10 nm [30] or higher, depending on the initial surface roughness, whereas the peak-to-peak height of the surface roughness of the induced morphology is in the range of 2–8 nm. Therefore, smoothing of the induced morphology requires lower fluences and an optimization of the fluences, and the number of steps and their energies can be performed to further reduce the final roughness and treatment time.
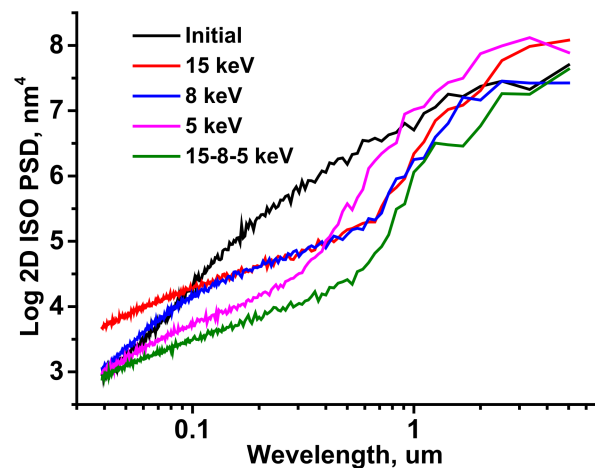
Figure 2. The 2D isotropic PSD functions of the Si surface after GCIB treatment at different energies.

4. Conclusions

A three-step energy treatment by Ar cluster ion beams was applied to improve the performance of the smoothing process of Si wafers. At the first step, at a higher energy of 15 keV, the cluster ions removed the initial morphological features (scratches). The next two steps (at 8 and 5 kV energies) were used to reduce the surface roughness that was introduced by the induced morphology that formed during the higher energy bombardment. To compare the smoothing performance, we also prepared three samples that were treated at 15, 8, and 5 keV at the same cluster ion beam fluences. The smoothing effect was estimated by the RMS roughness R_q and 2D isotropic power spectral density function. It was shown that single-step 15 keV treatment is effective to remove surface scratches; however, it creates induced surface morphology. The latter effect resulted in no change in roughness within the experimental uncertainty. The R_q before and after 15 keV treatment was 1.69 and 1.64 nm, respectively. Lower single-step energy treatments demonstrated a better smoothing effect. However, the fluence of a 5 keV treatment, due to lower sputtering rate, is insufficient to remove the initial scratches. The three-step process combines the advantages of a high energy treatment, which effectively removes the scratches, and a low energy treatment, which forms less developed induced surface morphology, and results in the lowest R_q roughness of 0.65 nm.

Author Contributions: Conceptualization, V.P. and A.T.; investigation, X.Z. (Xiaomei Zeng) and X.Z. (Xiangyu Zhang); visualization, X.Z. (Xiaomei Zeng) and Y.L.; formal analysis, V.P., X.Z. (Xiaomei Zeng) and A.T.; writing—original draft preparation, X.Z. (Xiaomei Zeng) and X.Z. (Xiangyu Zhang); writing—review and editing, V.P., A.T., Y.L., D.F. and B.Y.; funding acquisition, D.F. and B.Y. All authors have read and agreed to the published version of the manuscript.

Institutional Review Board Statement: Not applicable.

Informed Consent Statement: Not applicable.

Data Availability Statement: Data sharing is not applicable to this article.

Conflicts of Interest: The authors declare no conflict of interest.

References

1. Yamada, I. Historical milestones and future prospects of cluster ion beam technology. *Appl. Surf. Sci.* **2014**, *310*, 77–88. [CrossRef]
2. Popok, V.N. Energetic cluster ion beams: Modification of surfaces and shallow layers. *Mater. Sci. Eng. R* **2011**, *72*, 137–157. [CrossRef]
3. Ieshkin, A.E.; Tolstoguzov, A.B.; Korobeishchikov, N.G.; Pelenovich, V.O.; Chernysh, V.S. Gas-dynamic sources of cluster ions for basic and applied research. *Physics-Uspekhi* **2022**, *65*, 677–705. [CrossRef]
4. Henkes, P.R.W.; Klingelhöfer, R. Micromachining with cluster ions. *Vacuum* **1989**, *39*, 541–542. [CrossRef]
5. MacCrimmon, R.; Hautala, J.; Gwinn, M.; Sherman, S. Gas cluster ion beam infusion processing of semiconductors. *Nucl. Instrum. Methods B* **2006**, *242*, 427–430. [CrossRef]
6. Toyoda, N.; Yamada, I. MgF$_2$ and LaF$_3$ thin film formation with gas cluster ion beam assisted deposition. *Surf. Coat. Technol.* **2007**, *201*, 8620–8623. [CrossRef]
7. Teo, E.J.; Toyoda, N.; Yang, C.; Bettiol, A.A.; Teng, J.H. Nanoscale smoothing of plasmonic films and structures using gas cluster ion beam irradiation. *Appl. Phys. A* **2014**, *117*, 719–723. [CrossRef]
8. Ieshkin, A.E.; Svyakhovskiy, S.E.; Chernysh, V.S. Fabrication of optically smooth surface on the cleavage of porous silicon by gas cluster ion irradiation. *Vacuum* **2018**, *148*, 272–275. [CrossRef]
9. Korobeishchikov, N.G.; Nikolaev, I.V.; Roenko, M.A. Effect of argon cluster ion beam on fused silica surface morphology. *Nucl. Instrum. Methods B* **2019**, *438*, 1–5. [CrossRef]
10. Song, J.H.; Choi, D.K.; Choi, W.K. Dependence of surface smoothing, sputtering and etching phenomena on cluster ion dosages. *Nucl. Instrum. Methods B* **2002**, *196*, 268–274. [CrossRef]
11. Ieshkin, A.; Kireev, D.; Ozerova, K.; Senatulin, B. Surface ripples induced by gas cluster ion beam on copper surface at elevated temperatures. *Mater. Lett.* **2020**, *272*, 127829. [CrossRef]
12. Smirnov, B.M. Fractal clusters. *Sov. Phys. Usp.* **1986**, *29*, 481–505. [CrossRef]
13. Toyoda, N.; Yamada, I. Evaluation of charge state of gas cluster ions by means of individual crater observations. *Nucl. Instrum. Methods B* **2013**, *307*, 269–272. [CrossRef]
14. Yamada, I.; Matsuo, J.; Toyoda, N.; Kirkpatrick, A. Materials processing by gas cluster ion beams. *Mater. Sci. Eng. R* **2001**, *34*, 231–295. [CrossRef]
15. Insepov, Z.; Yamada, I. Molecular dynamics study of shock wave generation by cluster impact on solid targets. *Nucl. Instrum. Methods B* **1996**, *112*, 16–22. [CrossRef]
16. Toyoda, N.; Kitani, H.; Hagiwara, N.; Aoki, T.; Matsuo, J.; Yamada, I. Angular distributions of the particles sputtered with Ar cluster ions. *Mater. Chem. Phys.* **1998**, *54*, 262–265. [CrossRef]
17. Matsuo, J.; Toyoda, N.; Yamada, I. Nanofabrication technology by gas cluster ion beams. *J. Vac. Sci. Technol. B* **1996**, *14*, 3951–3954. [CrossRef]
18. Popok, V.N.; Prasalovich, S.V.; Campbell, E.E.B. Surface nanostructuring by implantation of cluster ions. *Vacuum* **2004**, *76*, 265–272. [CrossRef]
19. Allen, L.P.; Fenner, D.B.; DiFilippo, V.; Santeufemio, C.; Degenkolb, E.; Brooks, W.; Mack, M.; Hautala, J. Substrate smoothing using gas cluster ion beam processing. *J. Electron. Mater.* **2001**, *30*, 829–833. [CrossRef]
20. Isogai, H.; Toyoda, E.; Senda, T.; Izunome, K.; Kashima, K.; Toyoda, N.; Yamada, I. Dependence of recovery of Si surface damaged by GCIB irradiation on annealing temperature. *Nucl. Instrum. Methods B* **2008**, *266*, 2533–2536. [CrossRef]
21. Ieshkin, A.; Kireev, D.; Chernysh, V.; Molchanov, A.; Serebryakov, A.; Chirkin, M. Decomposition of AFM images of ultrasmooth optical surface polished with gas cluster ion beam. *Surf. Topogr. Metrol. Prop.* **2019**, *7*, 025016. [CrossRef]
22. Toyoda, N.; Hagiwara, N.; Matsuo, J.; Yamada, I. Surface smoothing mechanism of gas cluster ion beams. *Nucl. Instrum. Methods B* **2000**, *161–163*, 980–985. [CrossRef]
23. Aoki, T.; Seki, T.; Matsuo, J. Molecular dynamics simulations for gas cluster ion beam processes. *Vacuum* **2010**, *84*, 994–998. [CrossRef]
24. Matsuo, J.; Ninomiya, S.; Nakata, Y.; Ichiki, K.; Aoki, T.; Seki, T. Size effect in cluster collision on solid surfaces. *Nucl. Instrum. Methods B* **2007**, *257*, 627–631. [CrossRef]
25. Averback, R.; Ghaly, M. MD studies of the interactions of low energy particles and clusters with surfaces. *Nucl. Instrum. Methods Phys. Res. B* **1994**, *90*, 191–201. [CrossRef]
26. Houzumi, S.; Mochiji, K.; Toyoda, N.; Yamada, I. Scanning Tunneling Microscopy Observation of Graphite Surfaces Irradiated with Size-Selected Ar Cluster Ion Beams. *Jpn. J. Appl. Phys.* **2005**, *44*, 6252–6254. [CrossRef]
27. Gspann, J. Microstructuring by nanoparticle impact lithography. *Sensor Actuator. A* **1995**, *51*, 37–39. [CrossRef]
28. Insepov, Z.; Manory, R.; Matsuo, J.; Yamada, I. Proposal for a hardness measurement technique without indentor by gas-cluster-beam bombardment. *Phys. Rev. B* **2000**, *61*, 8744–8752. [CrossRef]
29. Seah, M.P. Universal Equation for Argon Gas Cluster Sputtering Yields. *Phys. Chem. C* **2013**, *117*, 12622–12632. [CrossRef]
30. Greer, J.A.; Fenner, D.B.; Hautala, J.; Allen, L.P.; DiFilippo, V.; Toyoda, N.; Yamada, I.; Matsuo, J.; Minami, E.; Katsumata, H. Etching, smoothing, and deposition with gas-cluster ion beam Technology. *Surf. Coat. Technol.* **2000**, *133–134*, 273–282. [CrossRef]
31. Seki, T.; Matsuo, J. Development of 1 mA cluster ion beam source. *Nucl. Instrum. Methods B* **2005**, *237*, 455–458. [CrossRef]

32. Pelenovich, V.O.; Zeng, X.M.; Ieshkin, A.E.; Chernysh, V.S.; Tolstogouzov, A.B.; Yang, B.; Fu, D.J. Development of a Gas Cluster Ion Source and Its Application for Surface Treatment. *J. Synch. Investig.* **2019**, *13*, 344–350. [CrossRef]
33. Mashita, T.; Toyoda, N.; Yamada, I. Surface Smoothing of Polycrystalline Substrates with Gas Cluster Ion Beams. *Jpn. J. Appl. Phys.* **2010**, *49*, 06GH09. [CrossRef]